Chemical Science

Accepted Manuscript

This article can be cited before page numbers have been issued, to do this please use: A. Austin-Kloppe, N. Degroot, B. Dhakal, J. Sager, L. Phan, S. Poormoghim and Y. Lu, *Chem. Sci.*, 2026, DOI: 10.1039/D6SC01847E.

ROYAL SOCIETY OF CHEMISTRY

rsc.li/chemical-science

View Article Online
DOI: 10.1039/D6SC01847E

Free Energy Relationship Analysis for Temperature Dependence of Hydride Kinetic Isotope Effects of NADH/NAD$^+$ Model Reactions: Implication for Barrier Compression by Enzyme Dynamics

Ava Austin-Kloppe,† Nicholas DeGroot,† Bikram Dhakal, Jessica Sager, Lauren Phan, Seyedmehrad Poormoghim, Yun Lu*
Department of Chemistry, Southern Illinois University Edwardsville, Edwardsville, Illinois 62026, United States

ABSTRACT:

Observed shift from temperature(T)-independence of hydrogen kinetic isotope effects (KIEs) in wild-type enzymes to T-dependence of KIEs in enzyme mutants has been explained as evidence for a role of protein dynamics in compressing donor(Don)-acceptor(Acc) distances (DADs) for catalysis. To test this explanation, correlation analysis between free energy changes ($\Delta G°$ = -44.3 to 6.7 kcal/mol) that simulate system rigidities and T-dependence of KIEs (represented by $\Delta E_a = E_{aD} - E_{aH}$) was carried out for 34 hydride-tunneling reactions of NADH/NAD$^+$ models in acetonitrile. For exergonic reactions, ΔE_a increases as $\Delta G°$ approaches zero, with the linear trend appearing to reverse for endergonic reactions. Both ΔE_a and KIE reach their maximum near thermoneutral reactions, where the charge-transfer (CT) complexation vibration is weakest and DAD is longest. A small portion of the free energy change drives the CT complexation vibrations and thus the DAD sampling that correlates to KIEs and their T-dependences. Results support the role of protein dynamics in barrier compression for catalysis. The new physical-organic linear ΔE_a–$\Delta G°$ relationship will contribute to the development of future H-tunneling models as well as updated theories for enzyme catalysis.

Introduction

Recent observations of temperature (T) independence (or weak dependence) of kinetic isotope effects (KIEs) in various enzyme-catalyzed hydrogen (H) transfer reactions have been ascribed by several research groups to the T-independence of narrowly distributed donor–acceptor distances (DADs) for H-tunneling processes.[1-14] Therefore, such observations are often cited in support of the proposed role of strong protein vibrational dynamics in facilitating short DAD sampling[1,15-20], and further promoting enzyme catalysis.[8,12,20-31] Use of this approach to propose the new physical origin of enzyme catalysis is currently, however, debated.[32-36] Central to the debate is whether T-dependence of KIEs reliably reflects DAD fluctuations or overall system rigidity. To address this question, biochemists have designed experiments to probe enzyme system rigidity and its correlation with the T-dependence of KIEs.[6,9,11,12,37-39] Theoreticians have refined or developed H-tunneling models to simulate the observations in attempts to test whether there is such a correlation.[14,32,33,40-43] For the same purpose, our group has studied model reactions in solution to explore potential relationship between structure and T-dependence of hydride KIEs.[24,25,27,29,44-50] The solution-phase H-transfer reactions permit systematic variation of molecular structure and solvent environment, enabling more controlled evaluation of how structural rigidity influences the T-dependence of KIEs in a broader context.

T-dependence of KIEs reflects the isotopic activation energy difference, represented as ΔE_a ($=E_{aD} - E_{aH}$) for hydrogen/deuterium transfer reactions. Semi-classically, ΔE_a falls within the range between 1.0–1.2 kcal/mol, but its relationship with structure is unpredictable. ΔE_a outside of this range has been used to suggest a H-tunneling mechanism. Notably, a shift from $\Delta E_a \sim 0$ in wild-type enzymes to $\Delta E_a > 0$ (often exceeding the semi-classical limit) in mutant variants has been frequently observed. This trend has prompted the application of existing H-tunneling models, as well as the development of new theoretical frameworks, to account for these observations and to further elucidate the mechanisms of H-transfer chemistry.[2,5-9,11,12,18,31,42,51-58] Among these, the recently proposed vibration-assisted activated H-tunneling (VA-AHT) model appears to be able to explain the unusual KIE behaviors.[2,5,8,20,59]

The VA-AHT model incorporates two orthogonal activation processes: (1) heavy atom motions bring the reactants (Donor-H and Acceptor) and products to degenerate energy states at which H-wave functions overlap ([Don-H↔H-Acc]‡), *i.e.*, tunnelling ready states (TRS's); and (2) more rapid heavy atom motions, also called promoting vibrations,[19,60] sample short DADs for efficient tunneling to occur. Since tunneling of a D-isotope requires a smaller average DAD due to its shorter de Broglie wavelength, a higher activation energy is needed leading to $E_{aD} > E_{aH}$ (assuming the first activation process is isotope insensitive). In wild-type enzymes, however, strong protein vibrations compress donor/acceptor closely together, thereby facilitating the formation of short DADs that are extremely densely populated, eliminating the possibility for further short DAD sampling for D-tunneling and making $\Delta E_a \sim 0$. In enzyme mutants, the constructive vibrations are disrupted, thermal sampling of shorter DADs is allowed so that T-dependence of DADs/KIEs ($\Delta E_a > 0$) emerges. The phenomenological model has been claimed by some researchers to be able to explain all of the hydrogen KIEs.[5,6,8,12]

Computational simulations of T-dependence of KIEs followed

View Article Online
DOI: 10.1039/D6SC01847E

various theoretical models including the VA-AHT model to investigate the proposed role of fast thermal dynamics in sampling short DADs. Other models include ensemble-averaged variational TS theory with multi-dimensional H-tunneling[32,41,61] as well as approaches using the empirical valence bond theory.[33,34,62] While the VA-AHT model has successfully reproduced the ΔE_a's in nonadiabatic reactions to support thermally activated DAD sampling concept,[63-65] simulations for more adiabatic hydride/proton transfer reactions has been challenging as there is not yet direct mathematical relationship between DADs and ΔE_a's for the type of reactions.[30,43] On the other hand, theoretical replications of the observations using other H-tunneling models, especially the huge KIEs, have encountered difficulty.[10,32,36,66] Nevertheless, even some of the latter computational results sometimes show that ΔE_a~0 in some reactions results from the insensitivity of DAD to temperature,[13,34,41,63] whereas other researchers have shown that it could also result from the effect of temperature on the microscopic mechanism, for example, on the position of the TS and shape of the potential barrier[32,34]. The potential relationship between DAD distributions and ΔE_a magnitudes warrants further investigation to search for a potential mathematical relationship, if exists, for building future H-tunnelling theoretical frameworks.

To address the "DAD–ΔE_a" relationship, additional data, including from model systems, are needed. Over the years, we have designed hydride transfer reactions of NADH/NAD$^+$ models in solution to tackle the problem. Our hypothesis, based on enzyme observations, is that a more rigid system with densely populated DADs gives rise to a smaller ΔE_a.[25] Systems have been designed to study the electronic, steric, and solvent effects as well as effects of remote heavy group vibrations and mechanisms on the T-dependence of KIEs.[25,27,29,44-50] Current results show that a tighter charge-transfer (CT) complexation between NADH/NAD$^+$ model structures exhibits a smaller ΔE_a value, supporting the hypothesis.

As the project progressed, we seemed to have identified a trend indicating that a reaction with more negative free energy change ($\Delta G°$) tends to show a smaller ΔE_a value.[29,44,46,48] This appears consistent with our hypothesis as a stronger hydride donor/acceptor would form stronger CT complexation vibrations and thus more rigid donor-acceptor centers. In this context, a larger negative $\Delta G°$ corresponds to a tighter CT complexation and, consequently, more densely populated smaller DADs, which in turn result in smaller ΔE_a values. Based on this reasoning, we envisioned that there might be a free energy relationship with T-dependence of KIEs for the type of reactions. As a matter of fact, according to a VA-AHT-inspired model, a portion of the free energy ($\Delta G°_{TRS}$) drives the structural and solvent rearrangement required to reach a TRS, while the remaining portion ($\Delta G°_{DAD}$) facilitates DAD sampling toward shorter distances; together, both contributions enable H-tunneling. While the overall free energy change ($\Delta G° = \Delta G°_{TRS} + \Delta G°_{DAD}$) is expected to linearly correlate with the logarithm of the observed rates (ln(k)), ΔE_a reflects (but is not equal to) the thermal energy required for DAD sampling and is expected to correlate linearly with the $\Delta G°_{DAD}$. Although $\Delta G°_{DAD}$ cannot be directly determined, establishing a ΔE_a–$\Delta G°$ relationship would provide an indirect means to test our DAD–ΔE_a hypothesis, clarify the driving force underlying ΔE_a, deepen our understanding of DAD sampling as well as the enzymatic KIE behavior.

In this work, we examined 34 hydride transfer reactions of NADH/NAD$^+$ models in acetonitrile, with $\Delta G°$ values spanning from −44.3 to 6.7 kcal/mol, to investigate the previously unreported ΔE_a–$\Delta G°$ relationship and further test our hypothesis concerning the DAD–ΔE_a relationship. We also compare the ΔE_a–$\Delta G°$ relationship with the ln(k)–$\Delta G°$ and ln(KIE)–$\Delta G°$ relationships. Furthermore, this study represents the first application of our hypothesis to endergonic reactions. The dataset reveals how the trends of these relationships evolve when transitioning from exergonic to endergonic regions. These insights enable testing of the DAD sampling mechanism in the VA-AHT model, evaluating other current H-transfer theories, as well as informing the development of future theoretical frameworks for both general H-transfer/tunneling reactions and enzyme catalysis.

Results

The hydride donor and acceptor structures are shown in Figure 1. Kinetics were determined spectroscopically on a stopped-flow

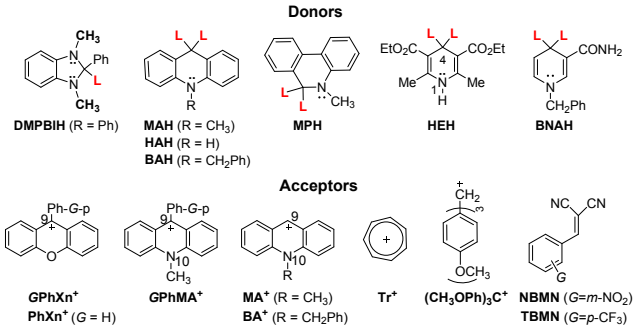

Figure 1. Hydride donors and acceptors (counter-ions: BF_4^-) (L = H or D) of the reactions in acetonitrile

UV-Vis spectrophotometer. The $\Delta G°$'s, second-order rate constants (k_2's) and KIEs at 25 ℃, as well as the ΔE_a values are listed in Table 1 (for Rxns **1** – **34**). As noted, some data was taken from our previous publications. Although kinetic study of the endergonic reactions is challenging due to limited extent of reaction and slow kinetics, in this work we were able to conduct the study on two such hydride transfer reactions: from Hantzsch 1,4-dihydropyridine (HEH) to benzylidenemalononitriles (BMNs), NBMN ($\Delta G°$ = 6.3 kcal/mol) and TBMN (6.7 kcal/mol) (Rxns **33** and **34** in Table 1, see structures in Figure 1). The reactions proceed to completion due to subsequent rapid irreversible transfer of a proton from the N-H site of the HE$^+$ product to the dicyanomethanide anion product, as illustrated below,[67]

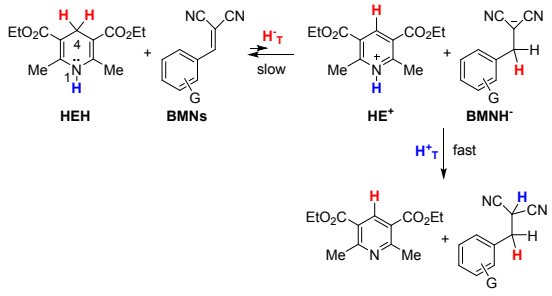

Table 1 also summarizes the relevant kinetic results for our previous study of the unfavorable hydride transfer reactions from alcohols (R^{1}CH(OH)R^2) to PhXn$^+$ in acetonitrile (Rxns **35**–**38**).[24,29]

View Article Online
DOI: 10.1039/D6SC01847E

Table 1. Hydride affinities ($-\Delta G°_{H^-}$), free energy changes ($\Delta G°$), and hydride transfer kinetic data in acetonitrile

Rxns	Donors (Don-H)	Hydride Acceptors ($Acc^+BF_4^-$)	$-\Delta G°_{H^-}(Don^+)$ [1] (kcal/mol)	$-\Delta G°_{H^-}(Acc^+)$ [1] (kcal/mol)	$\Delta G°$ (kcal/mol)	$k_{2H}(25°C)$ [1] ($M^{-1}s^{-1}$)	KIE(25°C) [m]	ΔE_a [m] (kcal/mol)
			Exergonic Reactions					
1 [a]	DMPBIH	CF_3PhXn^+	49.2	93.5	-44.3	1.44(0.01)x10^5	2.56 (0.03)	0.03 (0.07)
2 [a]	DMPBIH	$BrPhXn^+$	49.2	92.5	-43.3	9.86(0.09)x10^4	2.55 (0.03)	0.07 (0.07)
3 [a]	DMPBIH	$PhXn^+$	49.2	91.6	-42.4	4.54(0.05)x10^4	2.68 (0.04)	0.27 (0.06)
4 [a]	DMPBIH	CH_3OPhXn^+	49.2	90.2	-41.0	2.08(0.02)x10^4	2.74 (0.03)	0.55 (0.06)
5 [a]	DMPBIH	$(CH_3)_2NPhXn^+$	49.2	86.7	-37.5	6.34(0.04)x10^2	2.89 (0.06)	0.50 (0.08)
6 [b]	DMPBIH	MA^+	49.2	76.2	-27.0	2.12(0.01)x10^2	3.57 (0.03)	0.43 (0.15)
7 [a]	MAH	CF_3PhXn^+	76.2	93.5	-17.3	1.03(0.01)x10^3	4.06 (0.04)	0.89 (0.07)
8 [a]	MAH	$BrPhXn^+$	76.2	92.5	-16.3	6.45(0.03)x10^2	4.04 (0.03)	0.89 (0.07)
9 [a]	MAH	$PhXn^+$	76.2	91.6	-15.4	4.10(0.03)x10^2	4.08 (0.03)	0.88 (0.05)
10 [a]	MAH	CH_3OPhXn^+	76.2	90.2	-14.0	1.56(0.01)x10^2	4.18 (0.04)	0.92 (0.16)
11 [a]	MAH	$(CH_3)_2NPhXn^+$	76.2	86.7	-10.5	4.34(0.03)	4.45 (0.05)	0.96 (0.18)
12 [c]	MAH	Tr^+	76.2	83.0	-6.8	4.01(0.02)	4.95 (0.12)	1.14 (0.10)
13 [c]	HAH	Tr^+	74.9	83.0	-8.1	7.33(0.05)x10	5.34 (0.04)	1.27 (0.09)
14 [c]	HAH	$PhXn^+$	74.9	91.6	-16.7	1.15(0.01)x10^3	4.19 (0.03)	0.88 (0.05)
15 [e]	BAH	$PhXn^+$	77.4	91.6	-14.2	3.79(0.02)x10^2	4.26 (0.03)	0.89 (0.05)
16 [e]	MPH	$PhXn^+$	65.7	91.6	-25.9	3.74(0.02)x10^3	3.18 (0.03)	0.71 (0.05)
17 [c]	MPH	CH_3OPhXn^+	65.7	90.2	-24.5	1.65(0.01)x10^3	3.28 (0.03)	0.63 (0.05)
18 [c, d]	BNAH	MA^+	59.3	76.2	-16.9	7.16(0.07)x10	4.59 (0.06)	1.14 (0.17)
19 [c]	BNAH	BA^+	59.3	77.4	-18.1	2.48(0.02)x10^2	3.75 (0.03)	0.82 (0.07)
20 [c]	BNAH	$(CH_3OPh)_3C^+$	59.3	88.6	-29.3	1.66(0.01)x10^5	2.80 (0.03)	0.75 (0.05)
21 [e]	BNAH	$(CH_3)_2NPhXn^+$	59.3	86.7	-27.4	5.62(0.04)x10^4	3.19 (0.03)	0.82 (0.04)
22 [e]	BNAH	$(CH_3)_2NPhMA^+$	59.3	67.4	-8.1	8.37(0.08)x10^{-1}	4.79 (0.06)	1.14 (0.21)
23 [b]	HEH	MA^+	64.4	76.2	-11.8	1.56(0.01)x10^2	4.92 (0.04)	0.99 (0.11)
24 [f]	HEH	BA^+	64.4	77.4	-13.0	5.73(0.03)x10^2	4.53 (0.04)	1.01 (0.12)
25 [c]	HEH	$(CH_3OPh)_3C^+$	64.4	88.6	-24.2	5.66(0.03)x10^3	3.64 (0.03)	0.88 (0.06)
26 [g]	HEH	CF_3PhMA^+	64.4	78.4	-14.0	2.74(0.03)x10	5.23 (0.05)	1.13 (0.19)
27 [g]	HEH	$BrPhMA^+$	64.4	75.8	-11.4	2.09(0.03)x10	5.20 (0.08)	1.32 (0.09)
28 [g]	HEH	$PhMA^+$	64.4	74.1	-9.7	1.37(0.08)x10	5.31 (0.04))	1.19 (0.07)
29 [g]	HEH	CH_3PhMA^+	64.4	72.8	-8.4	1.13(0.02)x10	5.30 (0.10)	1.33 (0.10)
30 [g]	HEH	CH_3OPhMA^+	64.4	71.7	-7.3	1.00(0.01)x10	5.11 (0.08)	1.31 (0.10)
31 [g]	HEH	$(CH_3)_2NPhMA^+$	64.4	67.4	-3.0	4.19(0.03)	5.09 (0.06)	1.27 (0.14)
32 [g]	HEH	$(CH_3)_2NPhXn^+$	64.4	86.7	-22.3	8.87(0.05)x10^4	3.56 (0.02)	0.86 (0.08)
			Endergonic Reactions					
33 [c]	HEH	NBMN	64.4	58.1	6.3	1.14(0.01)	5.13 (0.06)	1.17 (0.15)
34 [c]	HEH	TBMN	64.4	57.7	6.7	6.07(0.02)x10^{-1}	5.27 (0.06)	1.19 (0.16)
35 [h]	BnOH	$PhXn^+$	- [j]	91.6	- [j]	6.73(0.29)x10^{-5} [k]	4.83 (0.21) [k]	1.00 (0.26)
36 [i]	*i*-PrOH	$PhXn^+$	- [j]	91.6	- [j]	2.02(0.05)x10^{-5} [k]	3.63 (0.23) [k]	0.83 (0.27)
37 [i]	*i*-PrOH-β,β-d_6	$PhXn^+$	- [j]	91.6	- [j]	2.01(0.05)x10^{-5} [k]	3.64 (0.16) [k]	0.80 (0.19)
38 [i]	*cyclo*-HexOH	$PhXn^+$	- [j]	91.6	- [j]	2.68(0.01)x10^{-5} [k]	3.68 (0.16) [k]	0.90 (0.27)

[a] Reference[44]; [b] Reference[25]; [c] This work; [d] ΔE_a = 1.53 (0.15) was reported by us before.[25] That was determined with temperatures from 4.5 – 29.5 °C, using the Hi-Tech Scientific SFA-20 fast kinetic determination kit interfaced to a UV-Vis spectrophotometer. The conclusions from that publication are not changed using the number obtained in this work; [e] Reference[48]; [f] Reference[29]; [g] Reference[47]; [h] Reference[24]; [i] Reference[29]; [j] Unreported; [k] For 22°C. [l] Reference[68]; [m] Numbers in paratheses are pooled standard deviations (standard deviations of the average values from different days of measurements in this work are listed in Tables S1 to S10 for comparison).

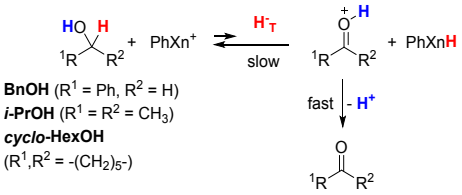

In these reactions, hydride-transfer from the α-position of the alcohol generates an α-hydroxy carbocation intermediate ($R^1C^+(OH)R^2$). This process is subsequently followed by rapid proton transfer of the OH group to basic species in solution (e.g., excess alcohol substrate or acetonitrile solvent), producing the corresponding oxidized carbonyl product ($R^1C(O)R^2$).[24,29,69-71]

While these extremely slow hydride transfer processes are expected to be endergonic, corresponding free energy data are not available in the literature, limiting quantitative free energy relationship analysis. Notably, these reactions proceed significantly more slowly than the endergonic reactions of HEH with BMNs (more than 10^4 times slower, see Table 1), suggesting that they would be even more endergonic. Estimated $\Delta G°$ values have therefore been obtained by extrapolating the linear $\ln(k_2)$–$\Delta G°$ correlation derived from reactions **1** – **34** (see Discussion section below). These estimates are included to support discussion of the trends observed across this limited set of endergonic reactions.

Discussion

Although the KIEs at 25 °C are all below 6, a majority of the ΔE_a values fall outside of the semiclassical range from 1.0 to 1.2 kcal/mol (Table 1). These results are consistent with observations from enzyme-catalyzed hydride transfer reactions involving NADH/NAD^+ coenzymes. In both enzymatic and solution systems,

View Article Online
DOI: 10.1039/D6SC01847E

such findings have been analyzed to suggest tunneling mechanisms.[5,48,72-74]

Free energy relationship analysis for T-dependence of KIEs: The Λ-shaped ΔE_a–$\Delta G°$ correlation

We first performed a linear correlation analysis for all 34 ln(k_2)–$\Delta G°$ data points (Figure 2**A**). Although the fit is poor (R^2 = 0.748), it reveals a clear trend that the reaction rate decreases as $\Delta G°$ becomes less negative within the exergonic region and continues to decrease as the reactions become endergonic. Analysis of the ΔE_a–$\Delta G°$ relationship shows a relatively good linear correlation for the 32 exergonic reactions (Figure 2**B** for Rxns **1** – **32**, $\Delta G°$ = -44.3 to -3.0 kcal/mol, R^2 = 0.852), whereas the two endergonic reactions appear as significant outliers. Within the exergonic region, the ΔE_a increases as $\Delta G°$ approaches zero. This new observation is consistent with our expectation; a more negative $\Delta G°$ corresponds to a more rigid system and a smaller ΔE_a, with a portion of $\Delta G°$ ($\Delta G°_{DAD}$) contributing to the activation process associated with DAD sampling.

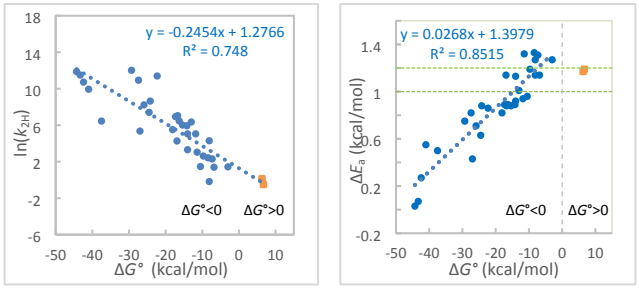

(A) **(B)**

Figure 2. (**A**) The linear fit of the ln(k_{2H})-$\Delta G°$ data for the 34 hydride transfer reactions (Rxns **1** – **34**). (**B**) The linear fit of the ΔE_a–$\Delta G°$ data for the 32 exergonic hydride transfer reactions in acetonitrile (Rxns **1** – **32**). The trend appears to turn to the opposite direction for endergonic reactions of BMNs (Rxns **33** – **34**). Area between the two horizontal green dotted lines represents the semiclassical range. The reactions **35-38** are not included in both plots (see text).

Therefore, the two endergonic reactions appear to align with the 32 exergonic reactions in the linear ln(k_2)–$\Delta G°$ correlation, whereas they appear as significant outliers relative to the linear ΔE_a–$\Delta G°$ correlation for the 32 exergonic reactions. In the latter case, ΔE_a reaches maximum when the negative $\Delta G°$ approaches zero, but upon entering the endergonic region, it begins to decrease. One may think that this behavior is resulted from the experimental error or from structural diversity among the reactants, where factors other than electronic effects, such as steric effects, can affect the CT complexation strength and, consequently, the DAD distributions. While we already restricted the structures to rings containing C, N, O that involve only 2p orbitals in CT complexation and the reactions to only one-step hydride transfers between two carbons, to further minimize the structural variability factor, we replotted the ln(k_2)–$\Delta G°$ and ΔE_a–$\Delta G°$ correlations using only the 12 reactions with a common hydride donor, HEH (Figures 3**A** and 3**B**, respectively). In both plots, the endergonic data points are clearly outliers.

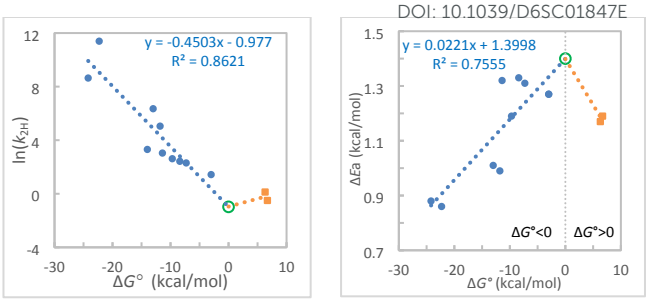

(A) **(B)**

Figure 3. (**A**) The linear fit of the ln(k_{2H})-$\Delta G°$ data for the 12 hydride transfer reactions with a common HEH hydride donor (Rxns **23** – **34**). (**B**) The linear fit of the ΔE_a–$\Delta G°$ data for the same 12 exergonic hydride transfer reactions. In both plots, the trend appears to turn to the opposite direction for endergonic reactions **33** – **34**. The empty green circle point in each plot is an extrapolated point at $\Delta G°$ = 0 derived from the linear equation from the exergonic reactions.

In Figure 3**A**, the two endergonic reactions appear to turn the linear ln(k_2)–$\Delta G°$ correlation derived from the exergonic reactions to the opposite direction. In Figure 3**B**, the two endergonic reactions clearly turn the linear ΔE_a–$\Delta G°$ correlation for the exergonic reactions to the opposite direction. Using the extrapolated $\Delta G°$=0 point from the exergonic reaction data (the circled points in Figures 3**A** and 3**B**), the corresponding linear correlations with the two data points from the endergonic reactions were drawn, which show a "V-shaped" ln(k_2)–$\Delta G°$ relationship and a "□-shaped" ΔE_a–$\Delta G°$ relationship.

We first discuss about the ΔE_a–$\Delta G°$ relationship (Figures 2**B** and 3**B**). Although the current analysis includes only two endergonic reaction data points, this trend could be reinforced by considering additional potential endergonic reactions **35** – **38**. While the $\Delta G°$ values are not available for these reactions, a qualitative assessment can still be performed. These $\Delta G°$ values could be approximately derived by substituting the corresponding k_2 values into the linear ln(k_2)–$\Delta G°$ correlation equation for the reactions **1** – **34** (Figure 2**A**). For one example, the k_2 for the reaction of BnOH with $PhXn^+$ in acetonitrile at 22℃ is 6.73 x 10^{-5} $M^{-1}s^{-1}$ (Table 1). Using our reported rate data at other temperatures[24] for an Arrhenius analysis, the rate constant at 25℃ is estimated to be 8.59 x 10^{-5} $M^{-1}s^{-1}$. Substituting the number to the linear fit equation from Figure 2**A** yields an estimated $\Delta G°$ = 43.4 kcal/mol, indicating a highly endergonic process. We recognize that such estimate could carry large uncertainty as the fit equation used depends upon many factors, such as dataset size, structural similarity among reactions, as well as experiment errors. Therefore, these estimated $\Delta G°$ values will not be used for quantitative analysis of the ΔE_a–$\Delta G°$ relationship. Nevertheless, the ΔE_a values for reactions **35** – **38** (0.80–1.00 kcal/mol) are significantly lower than those of the two endergonic reactions (**33** – **34**; ~1.2 kcal/mol). These observations support the conclusion that the ΔE_a–$\Delta G°$ trend for endergonic reactions is opposite to that observed for exergonic reactions.

The key question is why the clear linear ΔE_a–$\Delta G°$ plot for the exergonic reactions reverses direction at $\Delta G°$~0. This observation is reminiscent of the Marcus inverted region. In fact, the weakest CT complexation (*i.e.*, the longest average DAD) at TRS is expected from thermoneutral reactions ($\Delta G°$=$\Delta G°_{DAD}$=0). This inference is based on the Hammond's postulate. For an exergonic reaction, the more negative $\Delta G°$ would correspond with a tighter TRS that resembles more reactive reactant structures, whereas for

View Article Online
DOI: 10.1039/D6SC01847E

an endergonic reaction, the more positive $\Delta G°$ would also correspond with a tighter TRS that, however, resembles more reactive products. Therefore, within the VA-AHT-inspired model, $\Delta G°$ can be a proxy for TRS rigidity and a □-shaped ΔE_a–$\Delta G°$ relationship is expected, with the maximum ΔE_a occurring near $\Delta G°$=0 where DAD is longest. Our experimental observations (Figure 2**B** plus considering the ΔE_a values of the endergonic reactions **35** – **38**) are largely consistent with this expectation. Therefore, not only the ΔE_a–$\Delta G°$ correlation derived from exergonic reactions but also the reversed ΔE_a–$\Delta G°$ relationship for endergonic reactions support our proposed DAD–ΔE_a relationship. *That is, a more flexible system with a longer average DAD and a $\Delta G°$ closer to zero exhibits a larger ΔE_a value, regardless of whether the reaction is exergonic or endergonic.*

It should be noted that steric effects can influence the DAD distributions and, consequently, the ΔE_a values. Increased steric crowding may enhance system rigidity, leading to a decrease in ΔE_a.[25] Conversely, steric hindrance may also physically separate the donor and acceptor, enhancing system flexibility and resulting in higher ΔE_a values. Therefore, variations in steric effects across different systems may contribute to the observed scatter in the correlation, in addition to experimental errors.

The ln(k_2)–$\Delta G°$ correlation is consistent with the □-shaped ΔE_a–$\Delta G°$ relationship

Another question arises as to why the ΔE_a's of the two endergonic reactions decrease (Figure 3**A**) but their rates increase (Figure 3**B**) as compared to their corresponding values at $\Delta G° = 0$. The question can also be answered by considering the two activation processes in the VA-AHT-inspired model, the TRS formation and DAD sampling process. Note that TRS formation involves both the structural (hybridization and charge) and solvation reorganizations. The observed k_2 is determined by both processes (driven by both $\Delta G°_{TRS}$ and $\Delta G°_{DAD}$) and can be expressed as $k_2 = (k_{2,TRS} \bullet k_{2,DAD})^{1/2}$ (or more generally, a weighted geometric mean), where $k_{2,TRS}$ is the rate of reaching TRS with correct donor-acceptor alignment and $k_{2,DAD}$ is the rate of sampling short DADs required for tunneling. Theoretically, ln(k_{TRS}) would correlate linearly with the $\Delta G°_{TRS}$ across both the exergonic and endergonic regions, which is, ln(k_{TRS}) decreases as $\Delta G°_{TRS}$ increases from negative through zero to positive values (Figure 4**A**). In contrast, ln(k_{DAD}) is expected to decrease as exergonic reactions approach thermoneutral reactions due to increasing DADs, but then increase as the reactions become more endergonic due to, however, decreasing DADs. In other words, a V-shaped ln(k_{DAD})–$\Delta G°_{DAD}$ relationship is expected (Figure 4**B**). Since the observed ln(k_2)–$\Delta G°$ correlation is the "sum" of the two relationships (**A** and **B**), the observed ln(k_2)–$\Delta G°$ correlation is expected to show a broken-line profile with a breaking point at $\Delta G° = 0$ (Figure 4**C**).

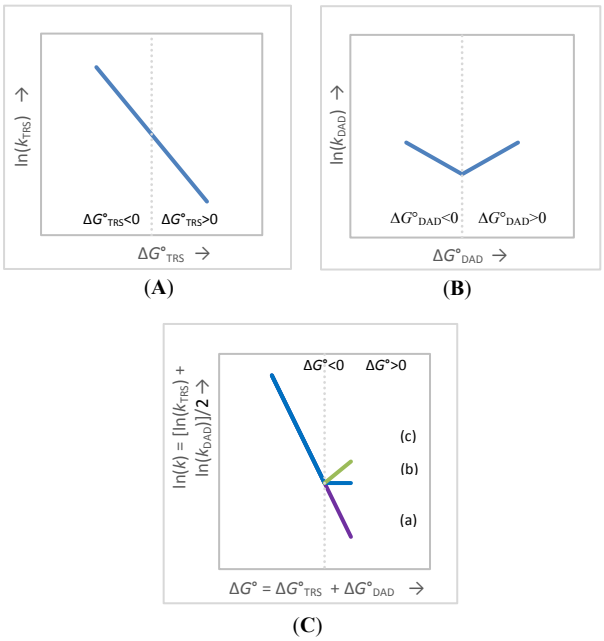

Figure 4. Predictions from the VA-AHT-inspired model for H-tunneling reactions. (**A**) the linear ln(k_{TRS})–$\Delta G°_{TRS}$ correlation involving both endergonic and exergonic reactions. (**B**) the V-shaped ln(k_{DAD})–$\Delta G°_{DAD}$ correlation with the turning point at $\Delta G°_{DAD} = 0$. (**C**) the overall ln(k)–$\Delta G°$ correlation that reflects the combined contributions of the plots **A** and **B**; Case (a): **A** is a steeper line or **B** is a shallow V-shape or both; from Cases (b) to (c): **A** becomes flatter or **B** becomes deeper or both. Note that the Λ-shaped ΔE_a–$\Delta G°_{DAD}$ relationship is another prediction from the model, mirroring the V-shaped ln(k_{DAD})–$\Delta G°_{DAD}$ correlation (but k_{DAD} is not directly experimentally accessible).

Theoretically, the pattern of the ln(k_2)–$\Delta G°$ correlation across exergonic and endergonic reactions depends upon the nature of the reaction systems, specifically, the steepness of the linear ln(k_{TRS})–$\Delta G°_{TRS}$ correlation and the depth of the V-shaped ln(k_{DAD})–$\Delta G°_{DAD}$ correlation. Figure 4**C**(a)–(c) describe three representative patterns. In (a), the ln(k_{TRS})–$\Delta G°_{TRS}$ linear correlation is steep while the V-shaped ln(k_{DAD})–$\Delta G°_{DAD}$ correlation is shallow, leading to only a slight deviation at $\Delta G° = 0$. From (b) to (c), the former correlation becomes less steep and/or the latter becomes deeper, leading to a more evident break and, ultimately a distinctly V-shaped profile. Therefore, all three patterns (a) to (c) are possible. Figure 3**A** presents the V-shaped ln(k_2)–$\Delta G°$ correlation (type (c) pattern). This correlation, along with the □-shaped ΔE_a–$\Delta G°$ correlation in Figure 3**B**, appears to support the two-coordinate mechanism proposed in the VA-AHT-inspired model.

It should be noted that patterns (b) and (c) in Figure 4**C** also resemble the Marcus inverted region. It is important, however, to note that relying solely on the ln(k)–$\Delta G°$ correlation to identify the DAD sampling mechanism needs caution as the bent or V-shaped ln(k_{DAD})–$\Delta G°_{DAD}$ relationship may be masked by the usually dominant and thus much steeper ln(k_{TRS})–$\Delta G°_{TRS}$ relationship. The latter relationship reflects structural rehybridization, charge redistribution, and solvent reorganization (pattern (a)), and thus contribute significantly to the activation process. Furthermore, the "bentness" of the ln(k)–$\Delta G°$ correlation depends on the relative linear correlations in between exergonic and endergonic regions. Each slope is influenced by factors such as electronic and steric properties, structural dynamics, the statistical size of the dataset, as well as experimental uncertainties. Consequently, failure to

View Article Online
DOI: 10.1039/D6SC01847E

observe a bent or V-shaped ln(k)–$\Delta G°$ correlation cannot preclude the existence of a DAD sampling mechanism. The apparently linear ln(k)–$\Delta G°$ correlation for all of the 34 reactions in Figure 2**A** most likely belongs to this situation. Nevertheless, simultaneous observation of both Λ-shaped ΔE_a–$\Delta G°$ relationship and V-shaped ln(k)–$\Delta G°$ relationship for the 12 reactions of HEH (Figure 3**B** versus 3**A**) provides strong support for our DAD–ΔE_a relationship hypothesis.

Therefore, Λ-shaped ΔE_a–$\Delta G°$ correlation and various patterns of ln(k_2)–$\Delta G°$ correlation are predicted by the VA-AHT-inspired model, and our experiments are consistent with these predictions. Note that observation of a Λ-shaped ΔE_a–$\Delta G°$ correlation does not guarantee that an evidently bent or V-shaped ln(k)–$\Delta G°$ correlation will also be observed. It should also be cautious to use a single bent or V-shaped ln(k_2)–$\Delta G°$ correlation to determine the DAD sampling mechanism.

The □-shaped ln(KIE)–$\Delta G°$ correlation is also consistent with the □-shaped ΔE_a–$\Delta G°$ relationship

With the KIE data in hand, we are also able to study the KIE–$\Delta G°$ correlation. Study of this relationship has had a long history. In 1960, Melander and Westheimer proposed that the maximum KIE should occur at $\Delta G° = 0$ where the transition state (TS) is symmetric.[75,76] Later, in 1980, Kresge deduced a parabolic relationship linking KIEs to $(\Delta G°)^2$ from the Marcus rate theory.[77] In the 1970s, Bell provided an alternative by introducing a tunnel correction to the one-dimensional energy barrier in the TS theory. In his model, tunneling probability is the greatest at a symmetrical TS, making the highest KIE, and it decreases as the TS becomes reactant- or product-like.[78] Since the 1980s, Kreevoy and coworkers studied the structure–KIE relationship for the hydride transfer reactions of NADH models in isopropanol/water using the Marcus rate theory that attributes a fraction of KIE to the corner-cutting tunneling mechanism.[72,74,79-81] Kil and Lee later found KIEs of a series of such exergonic hydride transfer reactions increase as $\Delta G°$ becomes less negative close to zero.[82] They used Kreevoy's treatment to explain their results and further predicted that the KIE–$\Delta G°$ relationship would reverse upon entering the endergonic region, which was, however, not yet been experimentally supported due to lack of the experiment data. Thus, this latter model also predicts a similar bell-shaped (or "upward/downward") dependence of KIEs on $\Delta G°$, with maximal tunneling and thus the largest KIE occurring near $\Delta G° \sim 0$, where the effective barrier is highest.

Within the VA-AHT-inspired model, KIE is defined differently. It is primarily dependent upon the difference in isotopic wave-function overlaps at the TRSs over a spectrum of DADs.[6,8,40,59] Because the vibrational wave-packet of H is more diffuse than that of D isotope, the H-overlap is more than the D-overlap so that KIE > 1.[40,83] (In other words, because D-tunneling requires shorter DADs than does H-tunneling,[40,83-86] $k_{D,DAD} < k_{H,DAD}$). Moreover, since the overlap for D-transfer decreases more rapidly than that for H-transfer with increasing DAD, KIE increases with DAD. (In other words, the difference between $k_{D,DAD}$ and $k_{H,DAD}$ becomes larger as DAD increases.) Consequently, KIE is predicted to be largest at $\Delta G° = 0$ where DAD is longest, and to decrease as TRS becomes reactant- or product-like where DAD shortens. Since the ln(k_{DAD})–$\Delta G°_{DAD}$ relationship is V-shaped (Figure 4**B**), and k_{TRS} is isotope insensitive, the ln(KIE)–$\Delta G°_{DAD}$ relationship is expected to be Λ-shaped.

We examine the ln(KIE)–$\Delta G°$ correlation to indirectly test the predicted Λ-shaped ln(KIE)–$\Delta G°_{DAD}$ relationship. The 34 ln(KIE)–$\Delta G°$ data points and the 12 such data points for the reactions of HEH only, are plotted in Figures 5**A** and 5**B**, respectively. Linear fits were applied separately to the exergonic and endergonic regions, with the $\Delta G° = 0$ point extrapolated from the exergonic data. In both plots, the endergonic reactions appear to reverse the trend observed for the exergonic reactions. The reverse trend could be further supported by including the smaller KIE values (3.63 – 4.83) from the endergonic reactions between alcohols and $PhXn^+$ (Rxns **35** – **38**), but again because of lack of corresponding $\Delta G°$ values these KIE data cannot be used for quantitative fitting analysis.

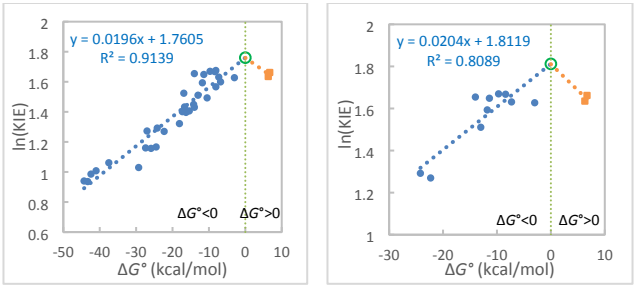

(A) **(B)**

Figure 5. (**A**) The linear fit of the ln(KIE(25°C))–$\Delta G°$ data for the 32 hydride transfer reactions. The reactions **35-38** are not included (see text). (**B**) The linear fit of the ln(KIE(25°C))–$\Delta G°$ data for the 12 hydride transfer reactions of a common hydride donor HEH (Rxns **23-34**). The empty green circle point in each plot is an extrapolated point at $\Delta G° = 0$ derived from the linear equation from the exergonic reactions.

The □-shaped ln(KIE)–$\Delta G°$ relationship is consistent with the □-shaped ΔE_a–$\Delta G°$ relationship in that both ΔE_a and KIE reach maxima near thermoneutral conditions (Figure 5 versus Figure 3**B**). Importantly, both relationships can be uniformly explained using the DAD coordinate mechanism within the VA-AHT-inspired model. According to this model, KIE increases with DAD. Note that previous studies on enzymatic reactions as well as NADH/NAD^+ model reactions have showcased this KIE–DAD relationship for exergonic reactions (Ref.[48] and references cited therein). Therefore, the maxima in both KIE and ΔE_a occurred near $\Delta G°$=0 correspond to longest DADs in H-tunneling mechanisms.

We noticed that the slopes of the ΔE_a–$\Delta G°$ (0.0268) and ln(KIE)–$\Delta G°$ (0.0196) correlations for the exergonic reactions are very small (Figures 2**B** and 5**A**). This likely reflects the fact that ΔE_a and ln(KIE) correlate only with the $\Delta G°$(DAD), which constitutes only a small fraction of the overall $\Delta G°$, so that they are much less sensitive to the overall $\Delta G°$.

Conclusions

Free-energy dependences of ΔE_a, rates (ln(k)), and ln(KIE) were analysed with 34 hydride tunneling reactions of NADH/NAD^+ models between two carbons in acetonitrile, which span both exergonic and endergonic regions. A clear linear ΔE_a–$\Delta G°$ relationship was, for the first time, observed for the exergonic reactions, with ΔE_a increasing as $\Delta G°$ approaches zero. Quantitative relationship has not yet been obtained for the limited number of endergonic reactions, but reversal of the trend from the exergonic reactions including reactions **35** – **38** has been clearly

View Article Online
DOI: 10.1039/D6SC01847E

shown. This is consistent with our hypothesis regarding the DAD–ΔE_a relationship. $\Delta G°$ (strictly, $\Delta G°_{DAD}$) acts as an indicator of system rigidity (or DAD distributions), where thermoneutral reactions correspond to most flexible and longest DADs. Overall, a portion of $\Delta G°$ of the reactions drive the CT complexation vibrations and thus DAD sampling, which is directly related to the T-dependence of KIEs. This resulting Λ-shaped ΔE_a–$\Delta G°$ relationship agrees with the prediction from the VA-AHT-inspired model that involves both the TRS formation and DAD sampling processes and attributes KIE to only the latter DAD sampling process.

The second prediction from the same model includes the bent- or V-shaped ln(k)–$\Delta G°$ relationship with the breaking/turning point at $\Delta G°$=0. It was found that the ln(k)–$\Delta G°$ plot is linear across the 34 reactions, but when using the data from the 12 reactions with a common hydride donor HEH, the V-shaped ln(k)–$\Delta G°$ relationship emerges, which mirrors the Λ-shaped ΔE_a–$\Delta G°$ relationship found from the same series of the reactions. The latter also appears to agree with the DAD sampling mechanism within the VA-AHT-inspired model.

The third prediction from the model includes the Λ-shaped ln(KIE)–$\Delta G°$ relationship. It was found that the ln(KIE)-$\Delta G°$ plot is linear across the 32 exergonic reactions, but when using the endergonic reactions, the correlation is reversed. This Λ-shaped trend is the same when using the 12 reactions of HEH. These results are consistent with the prediction. Therefore, all of the three predictions from the VA-AHT-inspired model, including the V-shaped ln(k)–$\Delta G°$, Λ-shaped ΔE_a–$\Delta G°$, and Λ-shaped ln(KIE)–$\Delta G°$ relationships, were simultaneously found in the 12 reactions of HEH, which support our DAD–ΔE_a relationship hypothesis.

Caution is required when using the ln(k)–$\Delta G°$ correlation alone to identify the DAD sampling mechanism as the expected bent- or V-shaped correlations can be largely masked by the dominant contribution from TRS formation, as well as by system selection and experimental uncertainties. Conversely, observation of the bent- or V-shaped ln(k)–$\Delta G°$ correlations alone should also be cautiously used to propose the DAD sampling mechanism, since $\Delta G°_{DAD}$ typically accounts for a small portion of the $\Delta G°$ so that system selection and experimental uncertainty need to be carefully considered. Also, a Λ-shaped ln(KIE)–$\Delta G°$ relationship alone should not be considered definitive evidence for DAD sampling either, since similar trends can arise from the Marcus theory combined with corner-cutting tunneling mechanism process, or even possibly from the classical Melander–Westheimer's "bond-stretching" model. In sharp contrast, the newly identified Λ-shaped ΔE_a–$\Delta G°$ relationship appearing to arise only from the DAD sampling could provide evidence for the DAD sampling mechanism; however, *whether or not this particular relationship is explainable by other tunnelling models remains unclear*.

The small slopes of the Λ-shaped ΔE_a–$\Delta G°$ and ln(KIE)–$\Delta G°$ relationships suggest that only a small portion of the $\Delta G°$ contributes to the activated DAD sampling process. The DAD increases as $\Delta G°$ of the exergonic reactions becomes less negative, becomes largest with thermoneutral reactions, and decreases as $\Delta G°$ becomes more positive in the endergonic reactions. This Λ-shaped ΔE_a–$\Delta G°$ relationship should be useful for evaluating the existing H-tunneling models and helping develop future H-transfer/tunneling theories.

Overall, our ΔE_a–$\Delta G°$ correlation results provide support for the DAD–ΔE_a relationship in the VA-AHT model (or the VA-AHT-inspired model); systems with more densely distributed small DADs give rise to smaller T-dependence of KIEs. Side-by-side comparison of solution-phase and enzymatic reactions on KIEs and their T-dependences suggests that frequently observed T-independence of KIEs from enzymes can be attributed to strong constructive fast protein dynamics that compress donor and acceptor close to each other for H-tunneling to occur. Therefore, there appears a synergy between C-H activation (for TRS formation and DAD sampling) and various protein dynamics (driven by $\Delta G°_{TRS}$ and $\Delta G°_{DAD}$) cooperatively functioning in enzymatic reactions.

Author Contributions

A. A.-K., N. D., B. D. and J. S. performed organic synthesis and kinetic measurements. A. A.-K. and N. D. wrote part of the paper. B. D. analyzed data. L. P. and S. P. performed organic synthesis. Y. L. designed research and wrote the manuscript.

AUTHOR INFORMATION

Corresponding Author

*** Yun Lu** – *Department of Chemistry, Southern Illinois University Edwardsville, Edwardsville, Illinois 62026, United States;* https://orcid.org/0000-0002-3511-6041; yulu@siue.edu

Authors

Ava Austin-Kloppe − *Department of Chemistry, Southern Illinois University Edwardsville, Edwardsville, Illinois 62026, United States*

Nicholas DeGroot − *Department of Chemistry, Southern Illinois University Edwardsville, Edwardsville, Illinois 62026, United States*

Bikram Dhakal − *Department of Chemistry, Southern Illinois University Edwardsville, Edwardsville, Illinois 62026, United States*

Jessica Sager − *Department of Chemistry, Southern Illinois University Edwardsville, Edwardsville, Illinois 62026, United States*

Lauren Phan − *Department of Chemistry, Southern Illinois University Edwardsville, Edwardsville, Illinois 62026, United States*

Seyedmehrad Poormoghim − *Department of Chemistry, Southern Illinois University Edwardsville, Edwardsville, Illinois 62026, United States*

Notes

The authors declare no competing financial interests.

† A.A. and N.D. contribute equally to both the experimental and writing of the manuscript.

Data Availability Statement

The data underlying this study are available in the published article and its Supplementary Information.

Supporting Information

Synthesis, procedures to determine the rate constants, T-dependence of KIEs plots, tabulated raw rate constants data, and the primary kinetic experiment data.

View Article Online
DOI: 10.1039/D6SC01847E

ACKNOWLEDGMENT

Acknowledgment is made to the donor of the National Institutes of Health (NIH R15 GM148951). We thank Pratichhya Adhikari (Southern Illinois University Edwardsville) for helping collect part of the kinetic data for the reaction of MPH with *p*-MeOPhXn$^+$, and Binita Maharajn and Peter Maness (from the same institution) for initial kinetic study of the reaction of MAH with Tr$^+$.

REFERENCES

(1) Kohen, A.; Cannio, R.; Bartolucci, S.; Klinman, J. P. Enzyme dynamics and hydrogen tunnelling in a thermophilic alcohol dehydrogenase. *Nature* **1999**, *399*, 496-499.

(2) Knapp, M. J.; Rickert, K.; Klinman, J. P. Temperature-dependent isotope effects in soybean lipoxygenase-1: Correlating hydrogen tunneling with protein dynamics. *J. Am. Chem. Soc.* **2002**, *124*, 3865-3874.

(3) Sikorski, R. S.; Wang, L.; Markham, K. A.; Rajagopalan, P. T. R.; Benkovic, S. J.; Kohen, A. Tunneling and coupled motion in the *E. coli* dihydrofolate reductase catalysis. *J. Am. Chem. Soc.* **2004**, *126*, 4778-4779.

(4) Loveridge, E. J.; Evans, R. M.; Allemann, R. K. Solvent Effects on Environmentally Coupled Hydrogen Tunnelling During Catalysis by Dihydrofolate Reductase from Thermotoga maritima. *Chemistry - A European Journal* **2008**, *14(34):10782-8*, 10782 - 10788.

(5) Nagel, Z. D.; Klinman, J. P. Update 1 of: Tunneling and dynamics in enzymatic hydride transfer. *Chem. Rev.* **2010**, *110*, PR41–PR67.

(6) Pudney, C. R. J., L.; Sutcliffe, M. J.; Hay, S.; Scrutton N. S. . Direct Analysis of Donor-Acceptor Distance and Relationship to Isotope Effects and the Force Constant for Barrier Compression in Enzymatic H-Tunneling Reactions. *J. Am. Chem. Soc.* **2010**, *132*, 11329-11335.

(7) Wang, Z.; Singh, P. N.; Czekster, M. C.; Kohen, A. S., V.L. Protein Mass-Modulated Effects in the Catalytic Mechanism of Dihydrofolate Reductase: Beyond Promoting Vibrations. *J. Am. Chem. Soc.* **2014**, *136*, 8333-8341.

(8) Kohen, A. Role of Dynamics in Enzyme Catalysis: Substantial vs. Semantic Controversies. *Acc. Chem. Res.* **2015**, *48*, 466-473.

(9) Romero, E.; Ladani, S. T.; Hamelberg, D.; Gadda, G. Solvent-Slaved Motions in the Hydride Tunneling Reaction Catalyzed by Human Glycolate Oxidase. *ACS Catal.* **2016**, *6*, 2113−2120.

(10) Klinman, J. P.; Offenbacher, A. R. Understanding Biological Hydrogen Transfer Through the Lens of Temperature Dependent Kinetic Isotope Effects. *Acc. Chem. Res.* **2018**, *51*, 1966–1974.

(11) Howe, G. W.; van der Donk, W. A. Temperature-Independent Kinetic Isotope Effects as Evidence for a Marcus-like Model of Hydride Tunneling in Phosphite Dehydrogenase. *Biochemistry* **2019**, *58*, 4260-4268.

(12) Singh, P.; Vandemeulebroucke, A.; Li, J.; Schulenburg, C.; Fortunato, G.; Kohen, A.; Hilvert, D.; Cheatum, C. M. Evolution of the Chemical Step in Enzyme Catalysis. *ACS Catal.* **2021**, *11*, 6726–6732.

(13) Hatcher, E.; Soudackov, A. V.; Hammes-Schiffer, A. Proton-Coupled Electron Transfer in Soybean Lipoxygenase: Dynamical Behavior and Temperature Dependence of Kinetic Isotope Effects. *J. Am. Chem. Soc.* **2007**, *129*, 187–196.

(14) Hu, S.; Soudackov, A. V.; Hammes-Schiffer, S.; Klinman, J. P. Enhanced Rigidification within a Double Mutant of Soybean Lipoxygenase Provides Experimental Support for Vibronically Nonadiabatic Proton-Coupled Electron Transfer Models. *ACS Catal.* **2017**, *7*, 3569−3574.

(15) Hammes-Schiffer, S.; Benkovic, S. J. Relating protein motion to catalysis. *Annu. Rev. Biochem.* **2006**, *75*, 519 – 541.

(16) Henzler-Wildman, K. A.; Lei, M.; Thai, V.; Kerns, S. J.; Karplus, M.; Kern, D. A Hierarchy of Timescales in Protein Dynamics Is Linked to Enzyme Catalysis *Nature* **2007**, *450*, 913−916.

(17) Hay, S.; Scruton, N. S. Good vibrations in enzyme-catalysed reactions. *Nature Chemistry* **2012**, *4*, 161-168.

(18) Klinman, J. P.; Kohen, A. Hydrogen Tunneling Links Protein Dynamics to Enzyme Catalysis. *Annu. Rev. Biochem.* **2013**, *82*, 471–496.

(19) Schramm, V. L.; Schwartz, S. D. Promoting vibrations and the function of enzymes. Emerging theoretical and experimental convergence. *Biochemistry* **2018**, *57*, 3299-3308.

(20) Klinman, J. P.; Miller, S. M.; Richards, N. G. J. A Foundational Shift in Models for Enzyme Function. *J. Am. Chem. Soc.* **2025**, *147*, 14884−14904.

(21) Hay, S.; Sutcliffe, M. J.; Scrutton, N. S. Promoting motions in enzyme catalysis probed by pressure studies of kinetic isotope effects. *Proc. Natl. Acad. Sci. U.S.A.* **2007**, *104*, 507-512.

(22) Bandaria, J.; Dutta, S.; Nydegger, M. W.; Rock, W.; Kohen, A.; Cheatum, C. Characterizing the dynamics of functionally relevant complexes of formate dehydrogenase. *Proc. Natl. Acad. Sci. USA.* **2010**, *107*, 17974-17979.

(23) Loveridge, E. J.; Tey, L.-H.; Allemann, R. K. Solvent Effects on Catalysis by Escherichia coli Dihydrofolate Reductase. *J. Am. Chem. Soc.* **2010**, *132*, 1137 – 1143.

(24) Liu, Q.; Zhao, Y.; Hammann, B.; Eilers, J.; Lu, Y.; Kohen, A. A Model Reaction Assesses Contribution of H-Tunneling and Coupled Motions to Enzyme Catalysis. *J. Org. Chem.* **2012**, *77*, 6825–6833.

(25) Lu, Y.; Wilhelm, S.; Bai, M.; Maness, P.; Ma, L. Replication of the Enzymatic Temperature Dependency of the Primary Hydride Kinetic Isotope Effects in Solution: Caused by the Protein Controlled Rigidity of the Donor-Acceptor Centers? *Biochemistry* **2019**, *58*, 4035–4046.

(26) Antoniou, D.; Schwartz, S. D. Role of protein motions in catalysis by Formate Dehydrogenase. *J. Phys. Chem. B* **2020**, *124*, 9483-9489.

(27) Bai, M.; Rijal, P.; Salarvand, S.; Lu, Y. Correlation of Temperature Dependence of Hydride Kinetic Isotope Effects with Donor-Acceptor Distances in Two Solvents of Different Polarities. *Org. Biol. Chem.* **2023**, *21*, 5090 – 5097.

(28) Schwartz, S. D. Protein Dynamics and Enzymatic Catalysis. *J. Phys. Chem. B* **2023**, *127*, 2649–2660.

(29) Singh, G.; Austin, A.; Bai, M.; Bradshaw, J.; Hammann, B. A.; Kabotso, D. E. K.; Lu, Y. Study of the Effects of Remote Heavy Group Vibrations on the Temperature Dependence of Hydride Kinetic Isotope Effects of the NADH/NAD+ Model Reactions. *ACS Omega* **2024**, *9*, 20593-20600.

(30) Hammes-Schiffer, S. Explaining Kinetic Isotope Effects in Proton-Coupled Electron Transfer Reactions. *Acc. Chem. Res.* **2025**, *58*, 1335−1344.

(31) Hu, S.; Offenbacher, A. R.; Thompson, E. M.; Gee, C. L.; Wilcoxen, J.; Carr, C. A. M.; Prigozhin, D. M.; Yang, V.; Alber, T.; Britt, R. D.; Fraser, J. S.; Klinman, J. P. Biophysical Characterization of a Disabled Double Mutant of Soybean Lipoxygenase: The "Undoing" of Precise Substrate Positioning Relative to Metal Cofactor and an Identified Dynamical Network. *J. Am. Chem. Soc.* **2019**, *141*, 1555-1567.

(32) Pu, J.; Ma, S.; Gao, J.; Truhlar, D. G. Small temperature dependence of the kinetic isotope effect for the hydride transfer reaction catalyzed by Escherichia coli dihydrofolate reductase. *J. Phys. Chem. B* **2005**, *109*, 8551−8556.

(33) Liu, H.; Warshel, A. Origin of the Temperature Dependence of Isotope Effects in Enzymatic Reactions: The Case of Dihydrofolate Reductase. *J. Phys. Chem. B* **2007**, *111*, 7852–7861.

(34) Kamerlin, S. C. L.; Warshel, A. An analysis of all the relevant facts and arguments indicates that enzyme catalysis does not involve large contributions from nuclear tunneling. *J. Phy. Org. Chem.* **2010**, *23*, 677-684.

(35) More O'Ferrall, R. A. Introduction to a symposium in print on tunnelling. *J. Phys. Org. Chem.* **2010**, *23*, 559-560.

(36) Truhlar, G. D. Tunneling in enzymatic and nonenzymatic hydrogen transfer reactions. *J. Phys. Org. Chem.* **2010**, *23*, 660-676.

(37) Wang, Z.; Kohen, A. Thymidylate synthase catalyzed H-transfers: Two chapters in one tale. *J. Am. Chem. Soc.* **2010**, *132*, 9820–9825.

(38) Ranasinghe, C.; Pagano, P.; Sapienza, P. J.; Lee, A. L.; Kohen, A.; Cheatum, C. M. Isotopic Labeling of Formate Dehydrogenase Perturbs the Protein Dynamics. *J. Phys. Chem. B* **2019**, *123*, 10403-10409.

(39) Horitani, M.; Offenbacher, A. R.; Marcus Carr, C. A.; Yu, T.; Hoeke, V.; Cutsail, G. E.; Hammes-Schiffer, S.; Klinman, J. P.; Hoffman, B. M. 13C ENDOR Spectroscopy of Lipoxygenase−Substrate Complexes Reveals the Structural Basis for C−H Activation by Tunneling. *J. Am. Chem. Soc.* **2017**, *139*, 1984−1997.

(40) Roston, D.; Kohen, A. Elusive transition state of alcohol dehydrogenase unveiled. *Proc. Nat. Acad. Sci. USA* **2010**, *107*, 9572-9577.

(41) Kanaan, N.; Ferrer, S.; Martí, S.; Garcia-Viloca, M.; Kohen, A.; Moliner, V. Temperature Dependence of the Kinetic Isotope Effects in

View Article Online
DOI: 10.1039/D6SC01847E

Thymidylate Synthase. A Theoretical Study. *J. Am. Chem. Soc.* **2011**, *133*, 6692–6702.
(42) Mhashal, A. R.; Major, D. T. Temperature-Dependent Kinetic Isotope Effects in R67 Dihydrofolate Reductase from Path-Integral Simulations. *J. Phys. Chem. B* **2021**, *125*, 1369–1377.
(43) Layfield, J. P.; Hammes-Schiffer, S. Hydrogen tunneling in enzymes and biomimetic models *Chem. Rev.* **2014**, *114*, 3466-3494.
(44) Maness, P.; Koirala, S.; Adhikari, P.; Salimraftar, N.; Lu, Y. Substituent Effects on Temperature Dependence of Kinetic Isotope Effects in Hydride-Transfer Reactions of NADH/NAD+ Analogues in Solution: Reaction Center Rigidity Is the Key. *Org. Lett.* **2020**, *22*, 5963–5967.
(45) Bai, M.; Koirala, S.; Lu, Y. Direct Correlation Between Donor-Acceptor Distance and Temperature Dependence of Kinetic Isotope Effects in Hydride-Tunneling Reactions of NADH/NAD+ Analogues. *J. Org. Chem.* **2021**, *86*, 7500–7507.
(46) Adhikari, P.; Song, M.; Bai, M.; Rijal, P.; DeGroot, N.; Lu, Y. Solvent Effects on the Temperature Dependence of Hydride Kinetic Isotope Effects: Correlation to the Donor–Acceptor Distances. *J. Phys. Chem. A* **2022**, *126*, 7675–7686.
(47) Beach, A.; Adhikari, P.; Singh, G.; Song, M.; DeGroot, N.; Lu, Y. Structural Effects on the Temperature Dependence of Hydride Kinetic Isotope Effects of the NADH/NAD+ Model Reactions in Acetonitrile: Charge-Transfer Complex Tightness Is a Key. *J. Org. Chem* **2024**, *89*, 3184–3193.
(48) Austin, A.; Sager, J.; Phan, L.; Lu, Y. Structural Effects on the Hydride-Tunneling Kinetic Isotope Effects of NADH/NAD+ Model Reactions: Relating to the Donor–Acceptor Distances. *J. Org. Chem.* **2025**, *90*, 3110-3115.
(49) Bai, M.; Singh, G.; Lu, Y. Rigidity Analysis of Hydride Tunneling Ready States from Secondary Kinetic Isotope Effects and Hammett Correlations: Relating to the Temperature Dependence of Kinetic Isotope Effects. *J. Phys. Org. Chem.* **2025**, *38*, DOI: 10.1002/poc.70002.
(50) Pokhrel, B.; Sager, J.; Adhikari, P.; Singh, G.; Dhakal, B.; Lu, Y. Large Temperature Dependence of Large Kinetic Isotope Effects of Multistep Hydride Reduction of p-Chloranil by NADH Models in Acetonitrile: Proton Tunneling within Loose Radical Ion-Pairs. *J. Org. Chem* **2025**, 16912-16917.
(51) Roston, D.; Cheatum, C. M.; Kohen, A. Hydrogen Donor-Acceptor Fluctuations from Kinetic Isotope Effects: A Phenomenological Model. *Biochemistry* **2012**, *51*, 6860-6870.
(52) Stojkoviç, V., Perissinotti, L., Willmer, D., Benkovic, S., and Kohen, A. Effects of the donor acceptor distance and dynamics on hydride tunneling in the dihydrofolate reductase catalyzed reaction. *J. Am. Chem. Soc.* **2012**, *134*, 1738-1745.
(53) Pagano, P.; Guo, Q.; Ranasinghe, C.; Schroeder, E.; Robben, K.; Häse, F.; Ye, H.; Wickersham, K.; Aspuru-Guzik, A.; Major, D. T.; Gakhar, L.; Kohen, A.; Cheatum, C. M. Oscillatory Active-Site Motions Correlate with Kinetic Isotope Effects in Formate Dehydrogenase. *ACS Catal.* **2019**, *9*, 11199−11206.
(54) Knapp, M. J.; Klinman, J. P. Environmentally coupled hydrogen tunneling. Linking catalysis to dynamics. *Eur. J. Biochem.* **2002**, *269*, 3113–3121.
(55) Agrawal, N.; Hong, B.; Mihai, C.; Kohen, A. Vibrationally Enhanced Hydrogen Tunneling in the *Escherichia coli* Thymidylate Synthase Catalyzed Reaction. *Biochemistry* **2004**, *43*, 1998-2006.
(56) Nagel, Z. D.; Meadows, C. W.; Dong, M.; Bahnson, B. J.; Klinman, J. P. Active Site Hydrophobic Residues Impact Hydrogen Tunneling Differently in a Thermophilic Alcohol Dehydrogenase at Optimal versus Nonoptimal Temperatures. *Biochemistry* **2012**, *51*, 4147−4156.
(57) Francis, K.; Sapienza, P.; Lee, A.; Kohen, A. The Effect of Protein Mass Modulation on Human Dihydrofolate Reductase. *Biochemistry* **2016**, *55*, 1100-1106.
(58) Geddes, A.; Paul, C. E.; Hay, S.; Hollmann, F.; Scrutton, N. S. Donor−Acceptor Distance Sampling Enhances the Performance of "Better than Nature" Nicotinamide Coenzyme Biomimetics. *J. Am. Chem. Soc.* **2016**, *138*, 11089−11092.
(59) Klinman, J. P. A new model for the origin of kinetic hydrogen isotope effects. *J. Phys. Org. Chem.* **2010**, *23*, 606–612.
(60) Roy, R. K.; Antoniou, D.; Schwartz, S. D. The Shaping of Enzymatic Free Energy Barriers through the Creation of Rate-Promoting Vibrations via Inter-Residue Cross-Talk on Multiple Time Scales. *J. Phys. Chem. B* **2025**, *129*, 9973−9982.
(61) Delgado, M. G., S.; Longbotham, J. E.; Scrutton, N. S.; Hay, S.; Moliner, V.; Tuñón, I. Convergence of Theory and Experiment on the Role of Preorganization, Quantum Tunneling, and Enzyme Motions into Flavoenzyme-Catalyzed Hydride Transfer. *ACS Catal.* **2017**, *7*, 3190–3198.
(62) Agarwal, P. K.; Billeter, S. R.; Rajagopalan, P. T. R.; Benkovic, S. J.; Hammes-Schiffer, S. Network of coupled promoting motions in enzyme catalysis. *Proc. Natl. Acad. Sci. USA* **2002**, *99*, 2794–2799.
(63) Hatcher, E.; Soudackov, A. V.; Hammes-Schiffer, S. Proton-coupled electron transfer in soybean lipoxygenase. *J. Am. Chem. Soc.* **2004**, *126*, 5763-5775.
(64) Salna, B.; Benabbas, A.; Russo, D.; Champion, P. M. Tunneling kinetics and nonadiabatic proton-coupled electron transfer in proteins: The effect of electric fields and anharmonic donor-acceptor interactions. *J. Phys. Chem. B* **2017**, *121*, 6869−6881.
(65) Li, P.; Soudackov, A. V.; Hammes-Schiffer, S. Fundamental insights into proton-coupled electron transfer in soybean lipoxygenase from quantum mechanical/molecular mechanics free energy simulations. *J. Am. Chem. Soc.* **2018**, *140*, 3068-3076.
(66) Pang, J.; Pu, J.; Gao, J.; Truhlar, D. G.; Allemann, R. K. Hydride Transfer Reaction Catalyzed by Hyperthermophilic Dihydrofolate Reductase Is Dominated by Quantum Mechanical Tunneling and Is Promoted by Both Inter- and Intramonomeric Correlated Motions. *J. Am. Chem. Soc.* **2006**, *128*, 8015-8023.
(67) Zhu, X.-Q.; Zou, H.-L.; Yuan, P.-W.; Liu, Y.; Cao, L.; Cheng, J.-P. A detailed investigation into the oxidation mechanism of Hantzsch 1,4-dihydropyridines by ethyl -cyanocinnamates and benzylidenemalononitriles. *J. Chem. Soc., Perkin Trans. 2* **2000**, 1857–1861.
(68) Shen, G. B.; Xia, K.; Li, X. T.; Li, J. L.; Fu, Y. H.; Yuan, L.; Zhu, X. Q. Prediction of Kinetic Isotope Effects for Various Hydride Transfer Reactions Using a New Kinetic Model. *J. Phys. Chem. A* **2016**, *120*, 1779−1799.
(69) Lu, Y., Qu, F., Moore, B., Endicott, D., Kuester, W. . Hydride Reduction of NAD+ Analogues by Isopropyl Alcohol: Kinetics, Deuterium Isotope Effects and Mechanism. *J. Org. Chem.* **2008**, *73*, 4763-4770.
(70) Lu, Y., Qu, F., Zhao, Y., Small, A. M., Bradshaw, J., Moore, B. Kinetics of the hydride reduction of an NAD(+) analogue by isopropyl alcohol in aqueous and acetonitrile solutions: solvent effects, deuterium isotope effects, and mechanism. *J. Org. Chem.* **2009**, *74*, 6503-6510.
(71) Lu, Y., Bradshaw, J., Zhao Y., Kuester, W., Kabotso D. . Structure–reactivity relationship for alcohol oxidations via hydride transfer to a carbocationic oxidizing agent. *J. Phys. Org. Chem.* **2011**, *24*, 1172–1178.
(72) Kreevoy, M. M.; Ostovic, D.; Truhlar, D. G. Phenomenological manifestations of large-curvature tunneling in hydride-transfer reactions. *J. Phys. Chem.* **1986**, *90*, 3766-3774.
(73) Kohen, A.; Klinman, J. P. Enzyme catalysis: beyond classical paradigms. *Acc. Chem. Res.* **1998**, *31*, 397-404.
(74) Han Lee, I.-S.; Jeoung, E. H.; Kreevoy, M. M. Primary Kinetic Isotope Effects on Hydride Transfer from 1,3-Dimethyl-2-phenylbenzimidazoline to NAD+ Analogues. *J. Am. Chem. Soc.* **2001**, *123*, 7492-7496.
(75) Melander, L.: In *Isotope Effects on Reaction Rates*; Ronald Press: New York, 1960; pp 24-32.
(76) Westheimer, F. H., 61, 265-73. THE mangitude of the Primary kinetic isotope effect for compounds of hydrogen and deuterium. *Chem. Rev.* **1961**, *61*, 265-273.
(77) Kreevoy, M. M. O., S.-W. Relation between rate and equilibrium constants for proton-transfer reactions. *J. Am. Chem. Soc.* **1973**, *95*, 4805-4810.
(78) Bell, R. P. Liversidge lecture. Recent advances in the study of kinetic hydrogen isotope effects. *Chem. Soc. Rev.* **1974**, *3*, 513-544.
(79) Kim, Y.; Truhlar, D. G.; Kreevoy, M. M. An experimentally based family of potential energy surfaces for hydride transfer between NAD+ analogs. *J. Am. Chem. Soc.* **1991**, *113*, 7837-7847.
(80) Kim, Y.; Kreevoy, M. M. The experimental manifestations of corner-cutting tunneling. *J. Am. Chem. Soc.* **1992**, *114*, 7116-7123.
(81) Lee, I.-S. H.; Jeoung, E. H.; Kreevoy, M. M. Marcus Theory of a Parallel Effect on R for Hydride Transfer Reaction between NAD+ Analogues. *J. Am. Chem. Soc.* **1997**, *119*, 2722-2728.
(82) Kil, H. J.; Lee, I.-S. H. Primary Kinetic Isotope Effects on Hydride Transfer from Heterocyclic Compounds to NAD + Analogues. *J. Phys. Chem. A* **2009**, *113*, 10704-10709.

View Article Online
DOI: 10.1039/D6SC01847E

(83) Roston, D.; Kohen, A. A Critical Test of the "Tunneling and Coupled Motion" Concept in Enzymatic Alcohol Oxidation. *J. Am. Chem. Soc.* **2013**, *135*, 13624–13627.
(84) Kashefolgheta, S.; Razzaghi, M.; Hammann, B.; Eilers, J.; Roston, D.; Lu, Y. Computational Replication of the Abnormal Secondary Kinetic Isotope Effects in a Hydride Transfer Reaction in Solution with a Motion Assisted H-Tunneling Model. *J. Org. Chem.* **2014**, *79*, 1989-1994.
(85) Maharjan, B.; Boroujeni, M. R.; Lefton, J.; White, O. R.; Razzaghi, M.; Hammann, B. A.; Derakhshani-Molayousefi, M.; Eilers, J. E.; Lu, Y. Steric Effects on the Primary Isotope Dependence of Secondary Kinetic Isotope Effects in Hydride Transfer Reactions in Solution: Caused by the Isotopically Different Tunneling Ready State Conformations? *J. Am. Chem. Soc.* **2015**, *137*, 6653 - 6661.
(86) Derakhshani-Molayousefi, M.; Kashefolgheta, S.; Eilers, J. E.; Lu, Y. Computational Replication of the Primary Isotope Dependence of Secondary Kinetic Isotope Effects in Solution Hydride-Transfer Reactions: Supporting the Isotopically Different Tunneling Ready State Conformations. *J. Phys. Chem. A* **2016**, *120*, 4277−4284.

View Article Online
DOI: 10.1039/D6SC01847E

Data Availability Statement

The data underlying this study are available in the published article and its Supplementary Information.